Chapter 3
Physics

Teiji Nishio

3.1 Electromagnetic Wave: X-Rays, Gamma Rays

Electromagnetic waves exhibit wave-particle duality, which means that they have the properties of both particles and waves. Photons travel at the speed of light, and their frequency ν, wavelength λ, and the speed of light c are related by the following equation:

$$\mathrm{c}[\mathrm{m/s}] = \lambda \cdot \nu = 3.0 \times 10^{8}. \tag{3.1}$$

The radiation used in radiation therapy includes high-energy X-rays and gamma rays, which are types of electromagnetic waves. Their energy in radiation therapy is expressed in the unit of MeV. The energy of an electromagnetic wave E is expressed by the following equation including Planck's constant h:

$$E[\mathrm{MeV}] = h \cdot \nu = \frac{h \cdot c}{\lambda} \approx 4.14 \times 10^{-21} \cdot \nu\left[\mathrm{s}^{-1}\right] \approx 1.24 \times 10^{-12}/\lambda[\mathrm{m}]. \tag{3.2}$$

As shown in Fig. 3.1, when matter is irradiated with an incident charged particle, an electromagnetic wave is released from outside of the nucleus in the form of an X-ray, while one is released by the nucleus in the form of a gamma ray. When the incident charged particle is an electron, bremsstrahlung is produced when the direction of the electron is deflected by the Coulomb force of the nucleus of the matter during its passage through the matter.

T. Nishio (✉)
Particle Therapy Division, Research Center for Innovative Oncology, National Cancer Center, 6-5-1 Kashiwanoha, Kashiwa-shi, Chiba 277-8577, Japan
e-mail: tnishio@east.ncc.go.jp

Y. Nagata (ed.), *Stereotactic Body Radiation Therapy*,
DOI 10.1007/978-4-431-54883-6_3

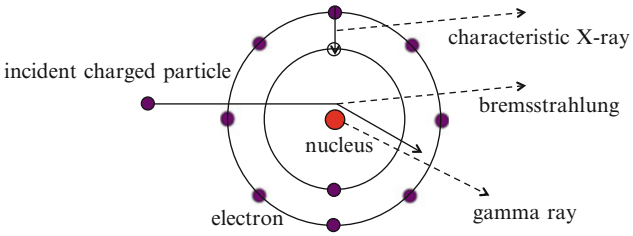

Fig. 3.1 The release of X-rays and gamma rays

Characteristic X-rays are electromagnetic radiation with a certain energy whose release corresponds to the filling of an outer-shell electron vacancy produced by the emission of an inner-shell electron of an atom of matter.

3.2 Interactions of Photons with Matter

Interactions of photons with matter depend on the energy of the photons. These interactions include the photoelectric effect, Rayleigh scattering (coherent scattering), Compton scattering (incoherent scattering), pair production, and photonuclear reaction. In radiation therapy, transfer of the energy possessed by photons to matter (i.e. a tumor) is important; it is necessary for this energy to be transferred from photons to electrons, which are charged particles. Therefore, the photoelectric effect, Compton scattering, and pair production are important interactions of photons with matter in radiation therapy (see Fig. 3.2).

3.2.1 Photoelectric Effect

The photoelectric effect is a reaction involving the loss of energy that is caused when photons of relatively low energy are absorbed by matter and bound electrons of atoms or molecules in that matter are released. The maximum kinetic energy E_e that is carried by an electron is given by the following equation. The term W is the work function, which means the minimum energy required to remove an electron from the binding of an atom or a molecule in the matter.

$$E_e \leq E - W, \quad E = h \cdot \nu. \tag{3.3}$$

The energy of a photon absorbed by the matter produces excitation of an atom; this excited atom then returns to its stable ground state by ejecting an Auger electron and an X-ray. Figure 3.3 shows the results of the mass attenuation coefficients $\mu_m = \mu/\rho$ for water, silver, and lead and the cross section as a function of the energy of the incident photon in the photoelectric effect [1]. The term ρ is the

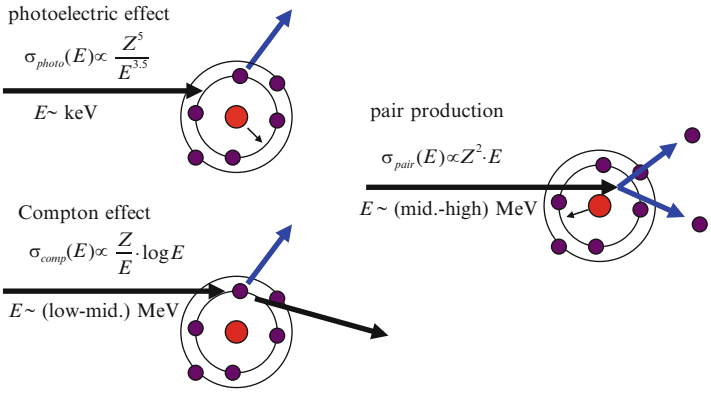

Fig. 3.2 The interactions of incident photons with matter

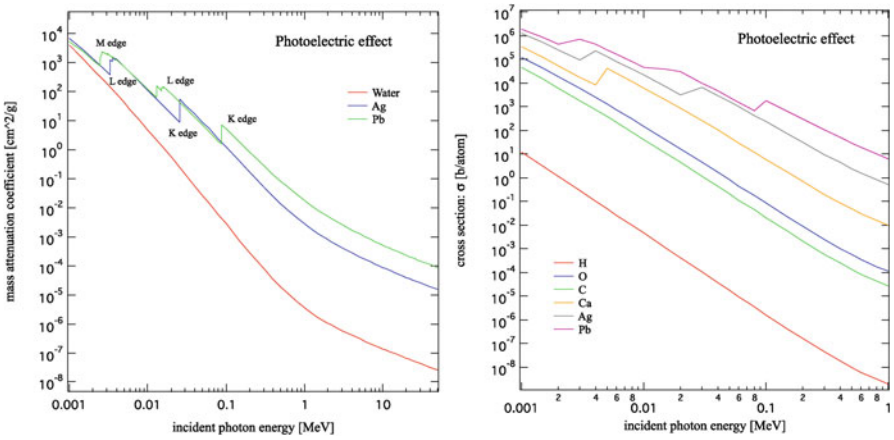

Fig. 3.3 The mass attenuation coefficient and the cross section as functions of the energy of the incident photon in the photoelectric effect [1]

density and μ is the attenuation coefficient. The photoelectric effect tends to emit inner-shell electrons (K-shell, L-shell, and M-shell), which are bound at a higher level of energy; in this regard, the effect causes a physical phenomenon in which an atom made unstable by absorption of the energy of a photon releases a high level of energy each time, but with a smaller number of reactions. As a result, the plot for the cross section of the photoelectric effect shows changes in a stepwise manner according to the bound energies of electrons (see Fig. 3.3).

The cross section of the photoelectric effect is approximately inversely proportional to the 3.5th power of energy of the incident photon and proportional to the 5th power of the atomic number of the matter. In addition, it is proportional to the 3.5th power of the effective atomic number of the matter.

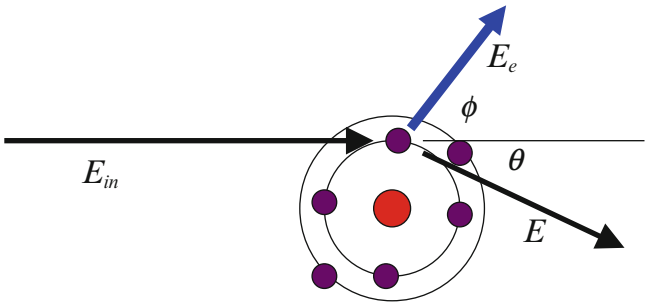

Fig. 3.4 The Compton effect

3.2.2 Compton Scattering

Compton scattering is a scattering phenomenon between a photon and an electron that is caused when the energy of the incident photon is much higher than the bound energy of the electron. The electron is given some of the energy of the incident photon and travels with that given energy as its kinetic energy, while the scattered photon loses energy. When the energy of the incident photon is far lower than the mass energy of the electron, the incident photon hardly loses energy by scattering with an electron. This phenomenon is called Thomson scattering. It is not necessary to consider this scattering phenomenon for photons with energy on the order of MeV, as used in radiation therapy.

As represented in Fig. 3.4, the following equation is given by the law of conservation of momentum and energy in Compton scattering:

$$\begin{aligned} E &= \frac{E_{in}}{1+\gamma\cdot(1-\cos\theta)}, \quad E_e = \frac{2\cdot\gamma\cdot\cos^2\phi}{(1+\gamma)^2-\gamma^2\cdot\cos^2\phi}, \\ \cot\left(\frac{\theta}{2}\right) &= (1+\gamma)\cdot\tan\phi, \quad \gamma = \frac{E_{in}}{m_e\cdot c^2}. \end{aligned} \tag{3.4}$$

where E_{in} is the energy of the incident photon, E is the energy of the scattered photon, θ is the scattering angle of the scattered photon, E_e is the energy of the recoil electron, and ϕ is the scattering angle of the recoil electron. The quantity of $m_e\cdot c^2 \approx 0.511[\mathrm{MeV}]$ is the rest mass energy of an electron. A recoil electron receives the maximum energy by Compton scattering when the scattering angle of the recoil electron $\phi = 0(\theta = \pi)$; and the following equation can then be derived from Eq. (3.4):

$$E_e \le E_e(\phi = 0) = E_{in}\cdot\frac{2\cdot\gamma}{1+2\cdot\gamma}. \tag{3.5}$$

The edge of the energy spectrum of a recoil electron with the maximum recoil energy is called the Compton edge. The difference between the wavelength of an

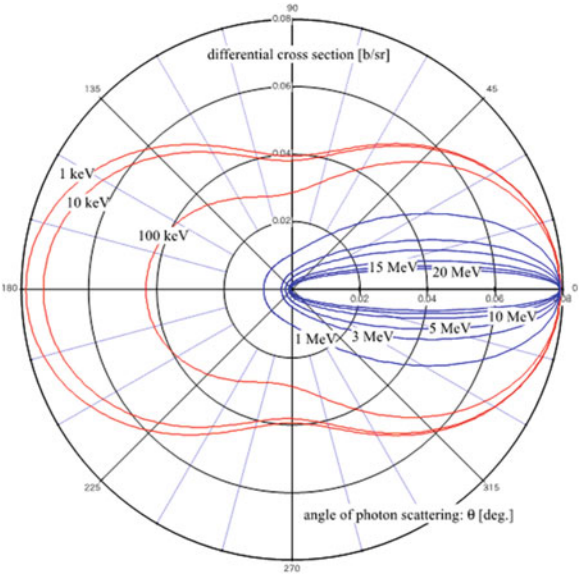

Fig. 3.5 The differential cross section of Compton scattering for every angle of a scattered photon as a function of the energy of the incident photon

incident photon and that of a scattered photon depends on the scattering angle θ, not on the energy of the incident photon or the scattered photon.

The differential cross section of Compton scattering per unit of solid angle is given by the Klein-Nishina formula:

$$\frac{d\sigma_{comp}(E_{in})}{d\Omega} = {r_e}^2 \cdot \frac{(1+\cos^2\theta)}{2\{1+\gamma\cdot(1-\cos\theta)\}^2} \times \left[1+\gamma^2\cdot\frac{(1-\cos\theta)^2}{(1+\cos\theta)^2\cdot\{1+\gamma\cdot(1-\cos\theta)\}}\right]. \tag{3.6}$$

$$r_e = \frac{e^2}{m_e\cdot c^2} \approx 2.818\times10^{-13}[cm]. \tag{3.7}$$

The term r_e is the classical electron radius. Figure 3.5 shows the results of calculation for the differential cross section of Compton scattering for every angle of a scattered photon as a function of the energy of the incident photon using Eqs. (3.6) and (3.7). The red lines in the figure represent the cases of incident photons with energy in the range of 1–100 keV, while the blue lines show those in the range of 1–10 MeV. As shown in the figure, the possibility of causing forward scattering increases when the energy of the incident photon becomes higher. This possibility is extremely high and Compton scattering tends to deposit energy of the incident photon forward for energy on the order of MeV (blue line in the figure), as used in radiation therapy.

The total cross section of Compton scattering σ_{comp} is given by integrating the differential cross section of Compton scattering (Eq. (3.6)) with the total solid angle. The result of the integral calculation is shown in Eq. (3.8).

$$\begin{aligned}\sigma_{comp}(E_{in}) &= \int_0^{4\cdot\pi} \left(d\sigma_{comp}(E_{in})/d\Omega\right) d\Omega \\ &= 2\cdot\pi\cdot {r_e}^2 \cdot \left[\frac{1+\gamma}{\gamma^2}\cdot\left\{\frac{2\cdot(1+\gamma)}{1+2\cdot\gamma} - \frac{1}{\gamma}\cdot\ln(1+2\cdot\gamma)\right\} + \frac{1}{2\cdot\gamma}\cdot\ln(1+2\cdot\gamma) - \frac{1+3\cdot\gamma}{(1+2\cdot\gamma)^2}\right].\end{aligned} \tag{3.8}$$

When the total cross section of Compton scattering is divided into the cross section of the Compton scattered photon σ_s and the cross section of the recoil electron σ_a, the following equation is given:

$$\sigma_{comp}(E_{in}) = \sigma_s(E_{in}) + \sigma_a(E_{in}). \tag{3.9}$$

$$\begin{aligned}\sigma_s(E_{in}) &= \int_0^{4\cdot\pi} \left[\{1+\gamma\cdot(1-\cos\theta)\}^{-1}\cdot\left(d\sigma_{comp}(E_{in})/d\Omega\right)\right] d\Omega \\ &= \pi\cdot {r_e}^2\cdot\left[\frac{1}{\gamma^3}\cdot\ln(1+2\cdot\gamma) + \frac{2\cdot(1+\gamma)\cdot(2\cdot\gamma^2-2\cdot\gamma-1)}{\gamma^2\cdot(1+2\cdot\gamma)^2} + \frac{8\cdot\gamma^2}{3\cdot(1+2\cdot\gamma)^3}\right].\end{aligned} \tag{3.10}$$

Figure 3.6 shows the results of calculation for the total cross section of the Compton scattering, the cross section of the Compton scattered photon and the cross section of the recoil electron as a function of the energy of the incident photon using Eqs. (3.8), (3.9), and (3.10). The figure shows that Compton scattering decreases as the energy of the incident photon increases.

3.2.3 Pair Production

Pair production is the phenomenon of the creation of a pair of an electron and a positron when an incident photon passes through a nearby atomic nucleus. Therefore, pair production does not occur in a vacuum. The generation of this phenomenon requires the energy of an incident photon to be greater than the total mass energy of an electron and a positron. In addition, the mass energy of an electron is the same as that of a positron. The total kinetic energy of an electron and that of a positron after pair production are expressed by the following equation because the recoil energy of an atom can be ignored in pair production.

$$E_+ + E_- = E_{in} - 2\cdot m_e\cdot c^2 = E_{in} - 1.022[\text{MeV}]. \tag{3.11}$$

The term E_- is the kinetic energy of an electron and E_+ is the kinetic energy of a positron. The kinetic energy of an incident photon is divided into an electron and a

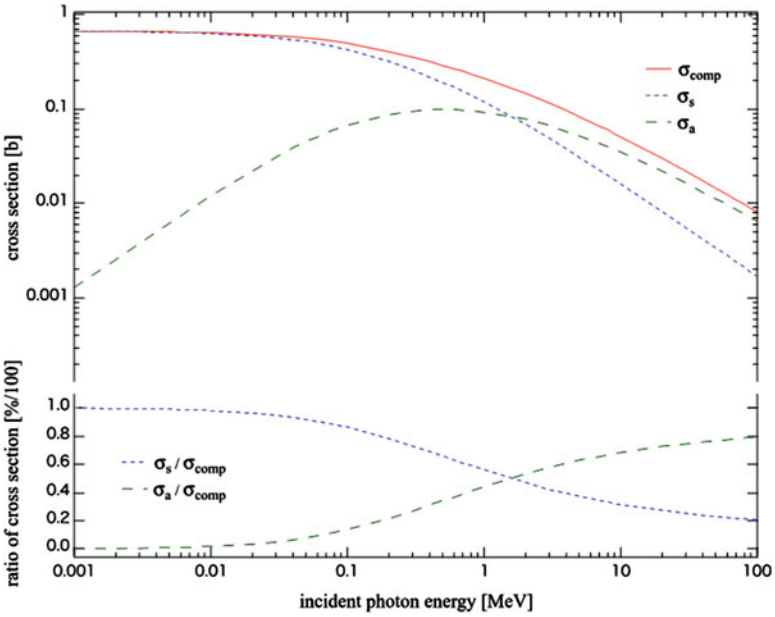

Fig. 3.6 The cross section of Compton scattering as a function of the energy of the incident photon

positron equally when the energy of the incident photon is low, while the division of the energy occurs unequally when the energy of the incident photon is high.

The cross section of pair production is zero in the case of the energy of an incident photon under the threshold energy 1.022 MeV, but it is proportional to the energy of an incident photon that is over this threshold. When the energy of an incident photon is high, the cross section increases slowly and is proportional to $\ln E_{in}$. It is also proportional to the second power of the atomic number of the matter.

3.3 Photon Flux in Matter

When a photon enters matter, the photon flux decreases by five interactions in matter: the photoelectric effect, Rayleigh scattering, Compton scattering, pair production, and photonuclear reaction. Figure 3.7 shows a schematic diagram of photon flux passing through matter. The relational equation is as follows:

$$I_{out} = I_{in} \cdot \exp(-\mu \cdot d), \tag{3.12}$$

where, d is the thickness of matter, I_{in} is the incident photon flux, I_{out} is the photon flux after passing through matter, and μ is the linear attenuation coefficient.

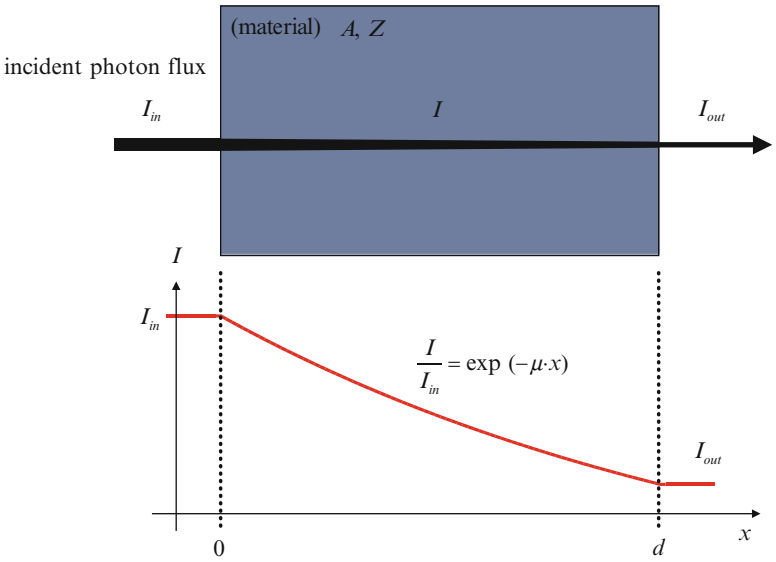

Fig. 3.7 Schematic diagram of photon flux upon passing through matter

The linear attenuation coefficient μ represents the amount of decrease per unit length in matter. It can approximate the total of the linear attenuation coefficient of the photoelectric effect μ_{phot}, Compton scattering μ_{comp}, and pair production μ_{pair} in the case of an incident photon with energy on the order of MeV, as used in radiotherapy.

$$\mu(E) = \sum_i \mu_i(E) \approx \mu_{phot}(E) + \mu_{comp}(E) + \mu_{pair}(E). \tag{3.13}$$

The relationship between the linear attenuation coefficient μ and the cross section σ for interactions of photons in matter is expressed by $\mu = n \cdot \rho$, using the density ρ and the number density of matter n. In addition, the number density can be expressed by $n = \rho \cdot N_A/A$ using the mass number A and Avogadro's constant N_A. Consequently, the linear attenuation coefficient is given by the following Eq. (3.14):

$$\mu(E) \approx \rho \cdot \frac{N_A}{A} \cdot \left(\sigma_{photo}(E) + Z \cdot \sigma_{comp}(E) + \sigma_{pair}(E)\right). \tag{3.14}$$

where, σ_{photo}, σ_{comp}, and σ_{pair} are the reaction cross section of the photoelectric effect, Compton scattering, and pair production, respectively.

Figure 3.8 shows the mass attenuation coefficient μ_m, which is calculated by dividing the linear attenuation coefficient μ by the density ρ, for each interaction as a function of the energy of the incident photon in water [1]. It can be observed from the figure that Compton scattering is a dominant interaction in the energy of X-rays

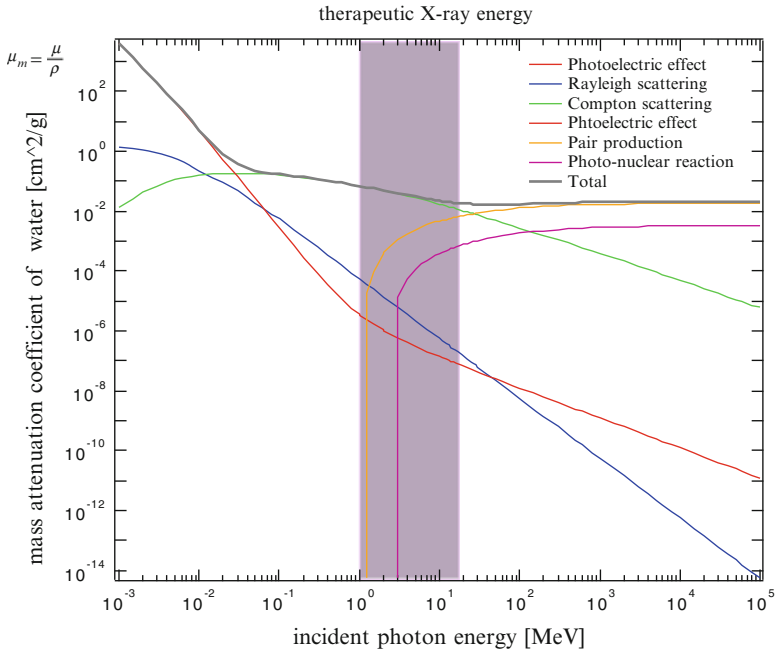

Fig. 3.8 The mass attenuation coefficient of water for each interaction as a function of the energy of the incident photon [1]

used in radiation therapy. The photoelectric effect and Compton scattering can occur almost equally in the energy range of X-rays of about 10–200 keV, as used in diagnostic radiation. Pair production is dominant in the case of very high energy.

Interactions of incident photons with matter cannot be described only by a simple model of attenuation of those photons because the energy distribution and the spatial distribution of the photons actually change in matter. For example, some incident photons become scattered photons, which are scattered forward after Compton scattering, and incident photons including those scattered photons undergo new interactions, especially in the range of energy used in radiation therapy. Therefore, the photon flux upon entering matter does not follow a simple exponential attenuation. Interactions of photons with real matter are very complicated, so it is necessary to consider the energy of the photon and its direction, as well as the mass attenuation coefficient of all energy and the photon flux at a point in the matter, as parameters of those interactions.

3.4 Energy Deposition by Incident Photons to Matter

An incident photon deposits kinetic energy E_e on an electron by interactions such as the photoelectric effect, Compton scattering, and pair production, and the electron deposits the energy on matter while passing through it (see Fig. 3.9). Stopping

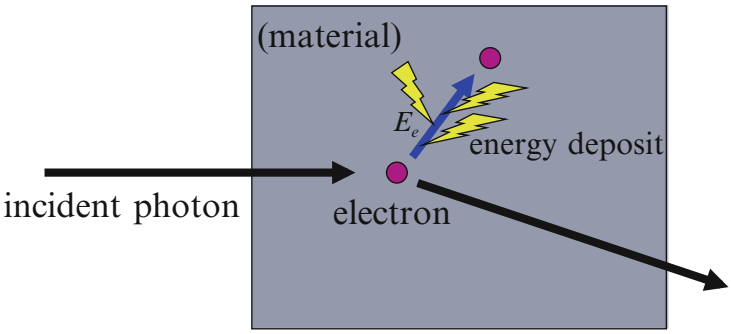

Fig. 3.9 Schematic diagram of energy deposition by an incident photon to matter

power is defined as the energy loss per length along the electron's track and is expressed as $-dE/dx[\mathrm{MeV/cm}]$. Mass stopping power $-dE/\rho \cdot dx[\mathrm{MeV \cdot cm^2/g}]$ is obtained by dividing the stopping power by the density of the matter.

Electron velocity while passing through matter is expressed by the following equation using an energy relational equation with special relativity:

$$\frac{m_e \cdot c^2}{\sqrt{1-\beta^2}} = E_e + m_e \cdot c^2. \quad \Rightarrow \quad \beta = \sqrt{1 - \frac{1}{(1 + E_e/m_e \cdot c^2)^2}}, \tag{3.15}$$

where, c is the speed of light, $\beta = v/c$, and e and m_e the electron charge and rest mass, respectively. $m_e \cdot c^2$ is the electron rest mass energy and its value is 0.511 MeV. The speed of an electron is above 50 % of the speed of light when the kinetic energy of the electron is only 0.08 MeV.

In terms of the mass-stopping power in the electron energy range that should be taken into consideration in radiation therapy, it can be divided into terms of ionization loss and radiation loss.

$$-\frac{dE_e}{\rho \cdot dx} = \left(-\frac{dE_e}{\rho \cdot dx}\right)_{col} + \left(-\frac{dE_e}{\rho \cdot dx}\right)_{rad}. \tag{3.16}$$

In Eq. (3.16), the first term represents ionization loss and the second represents radiation loss.

The term of an ionization loss is calculated using the Bethe-Bloch formula which describes the stopping power as follows:

$$\left(-\frac{dE_e}{\rho \cdot dx}\right)_{col} = \frac{2 \cdot \pi \cdot m_e \cdot c^2}{\beta^2} \cdot {r_e}^2 \cdot N_A \cdot \frac{Z}{A}$$
$$\times \left\{ \ln\left(\frac{2 \cdot m_e \cdot c^2 \cdot E_e \cdot \beta^2}{(1-\beta^2) \cdot I^2}\right) + (1-\beta^2) - \left(2 \cdot \sqrt{1-\beta^2} - 1 + \beta^2\right) \cdot \ln 2 + \frac{1}{8} \cdot \left(1 - \sqrt{1-\beta^2}\right)^2 \right\}, \tag{3.17}$$

where, N_A is the Avogadro's constant and I is the mean excitation potential energy. I for water is 75.0 eV. The term of an ionization loss is in proportional to the atomic number of the matter and inversely proportional to the electron energy.

Similarly, the term of a radiation loss is expressed as follows:

$$\left(-\frac{dE_e}{\rho \cdot dx}\right)_{rad} = \frac{E_e + m_e \cdot c^2}{\beta^2} \cdot \alpha \cdot {r_e}^2 \cdot N_A \cdot \frac{Z^2}{A} \cdot \left\{4 \cdot \ln\left(\frac{2 \cdot (E_e + m_e \cdot c^2)}{m_e \cdot c^2}\right) - \frac{4}{3}\right\}. \tag{3.18}$$

where, α is the fine-structure constant and has a constant value.

$$\alpha = \frac{e^2}{\hbar \cdot c} \approx \frac{1}{137}. \tag{3.19}$$

The term of a radiation loss is in proportional to the second power of the atomic number of the matter and to the electron energy.

The electron energy at which ionization loss is equal to radiation loss is called the critical energy E_c and is approximated by the following equation:

$$\left(-\frac{dE_e}{\rho \cdot dx}\right)_{col} = \left(-\frac{dE_e}{\rho \cdot dx}\right)_{rad} . \Rightarrow E_e = E_c \approx \frac{800}{Z + 1.2}[\text{MeV}]. \tag{3.20}$$

The critical energy for water is about 92 MeV using Eq. (3.20).

The results of calculation of the electron-stopping power in water by Eqs. (3.15), (3.16), (3.17), (3.18), and (3.19) are shown in Fig. 3.10. Radiation loses electron-stopping power predominantly in the energy range used in radiation therapy. The distance over which electron energy is $1/e$ due to the loss of almost all of its energy is called the radiation length L_{rad} and that of water is about 36 cm.

The mass of an electron is very small, at only about 1/1,800 that of a proton. Because an electron has a negative elementary electric charge, it is scattered markedly by Coulomb scattering in matter. In addition, an electron is scattered numerous times: this effect is called multiple Coulomb scattering. The term $\langle {\theta_e}^2 \rangle$ denotes the mean square angle of an electron for multiple Coulomb scattering and is given by the following equation:

$$\sqrt{\langle {\theta_e}^2 \rangle} \propto \frac{Z^2}{\beta^2} \cdot \frac{d}{L_{rad}}. \tag{3.21}$$

This equation shows that electron scattering in matter is proportional to the second power of the atomic number of the matter and to the thickness of the matter, while it is inversely proportional to the second power of the speed of an electron and to the radiation length of the matter. Because the speed of the recoil electron that is produced by Compton scattering with X-rays used in radiation therapy is almost

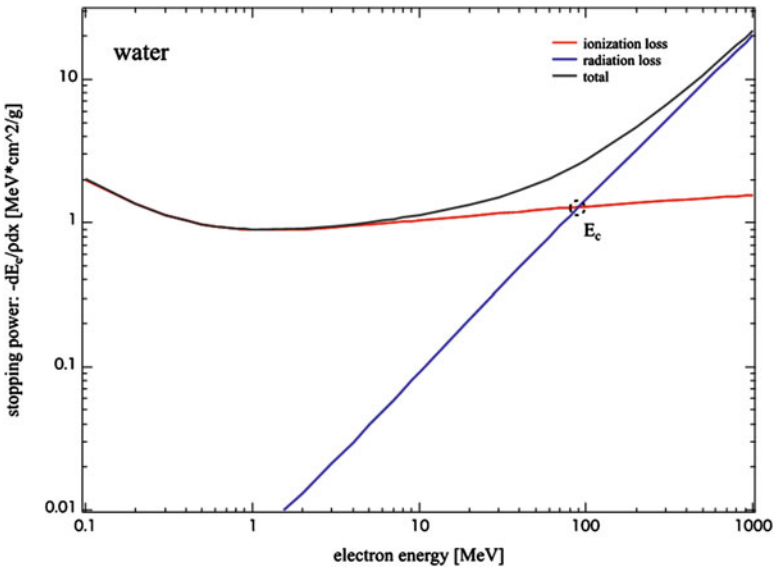

Fig. 3.10 The mass-stopping power for water as a function of electron energy

that of light in the range of kinetic energy of the recoil electron, the ratio of change of the scattering angle is small, at about 10 %.

The range of an electron in matter $R_e \cdot \rho$ can be calculated by integrating the reciprocal of mass-stopping power with electron energy from E_0 to zero, and can be expressed by the following equation:

$$R_e \cdot \rho = \int_{E_0}^{0} \left(-\frac{dE_e}{\rho \cdot dx} \right)_{col}^{-1} dE_e \left[\mathrm{g/cm^2} \right]. \tag{3.22}$$

However, the actual stopping positions of electrons diverge markedly because the electrons pass through matter while changing their directions in complicated ways by multiple Coulomb scattering. Therefore, the calculation results of Eq. (3.22) give electron path lengths in matter.

The energy deposition by electrons to matter that occurs when the X-rays used in radiation therapy irradiate matter is almost entirely due to energy losses of recoil electrons by Compton scattering. In addition, dose kernel K_X is formed by the energy losses of recoil electrons by Compton scattering at a point in matter.

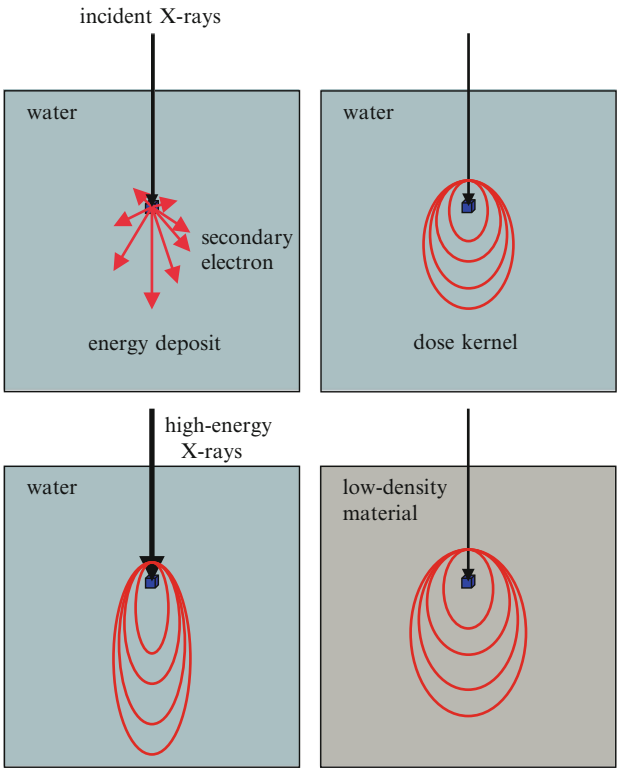

Fig. 3.11 Schematic diagram of shapes of dose kernels in various situations

$$K_X = K_X\left(\frac{d\sigma_{photo}}{d\Omega}, \frac{d\sigma_{comp}}{d\Omega}, \frac{d\sigma_{pair}}{d\Omega}\right) \approx K_X\left(\frac{d\sigma_{comp}}{d\Omega}\right) \approx K_X\left(\frac{d\sigma_a}{d\Omega}\right). \tag{3.23}$$

The shape of dose kernel K_X depends on the differential cross sections of recoil electrons following the Klein-Nishina formula (3.6). As shown in Fig. 3.11, the shape of dose kernel K_X is elongated forward in the case of incident photons or X-rays with high energy. In low-density matter, the shape of dose kernel K_X expands on the basis of its similarity. The shape of dose kernel K_X expands in a manner depending on the lung density in radiation therapy, whereas the shape in inhomogeneous matter is formed in a boundary region between the high-density area and the low-density area corresponding to the area between the mediastinum and the lungs because of a change in the shape under various conditions, such as incident energy and matter density. Dose distribution is given by convoluting dose kernel K_X within the spatial region inside matter that is irradiated by X-rays used in radiation therapy (see Fig. 3.12).

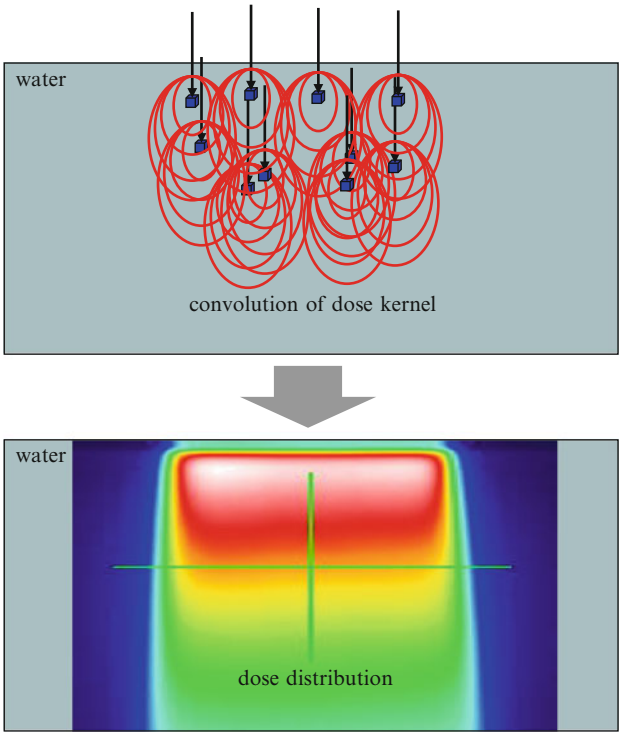

Fig. 3.12 An example of the dose distribution of X-rays used in radiation therapy

3.5 Energy Spectrum and Dose Distribution of Therapeutic X-Rays from a Linear Accelerator (Linac)

A linear accelerator (Linac) is used for X-ray therapy including stereotactic body radiation therapy (SBRT) for the lungs and the liver. Bremsstrahlung X-rays are produced by the phenomenon of bremsstrahlung, which occurs when MeV-energy electrons accelerated by a Linac irradiate a metallic target. Figure 3.13 shows the calculation results of the mass-stopping power for a tungsten (chemical symbol W) target as a function of electron energy. Compared with water (Fig. 3.10), the ratio of bremsstrahlung, which means the radiation loss in mass-stopping power, is larger for electrons with MeV-order energy, as used in radiation therapy. The critical energy for water is about 92 MeV; on the other hand, that for tungsten is small, at about 10 MeV.

Energy spectra of X-rays via bremsstrahlung by a Linac are formed by not only the incident energy of electrons to the target but also the material of the target or a flattening filter and their optical arrangement. Therefore, shapes of the energy spectra differ among Linac manufacturers. Typical energy spectra of X-rays of a Linac are shown in Fig. 3.14 [2].

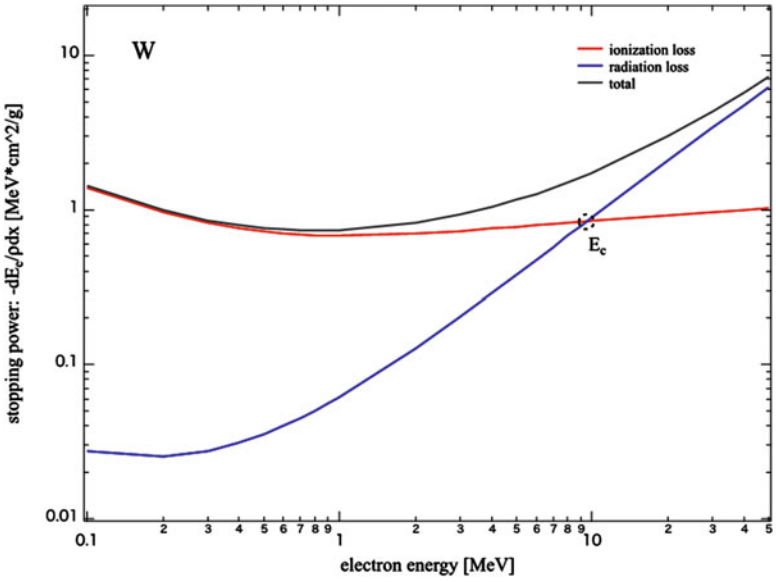

Fig. 3.13 The mass-stopping power for tungsten as a function of electron energy

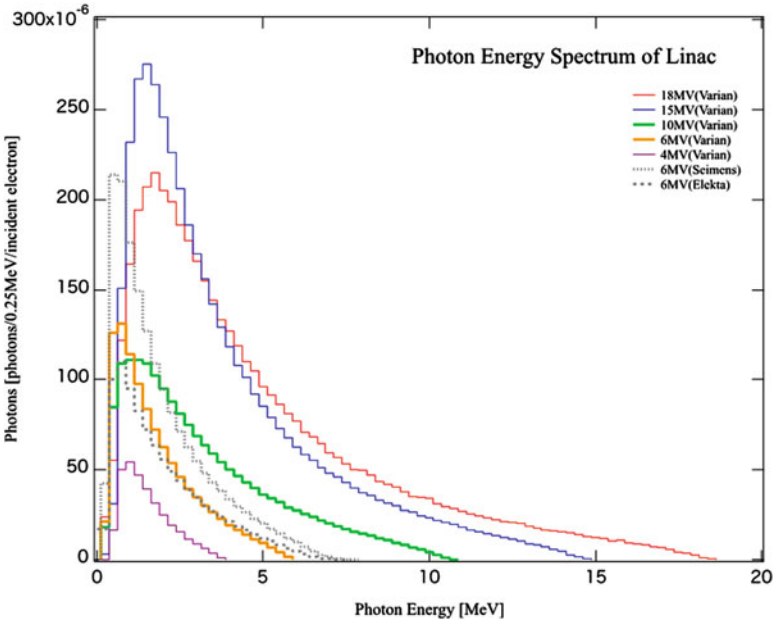

Fig. 3.14 The X-ray energy spectra of Linac [2]

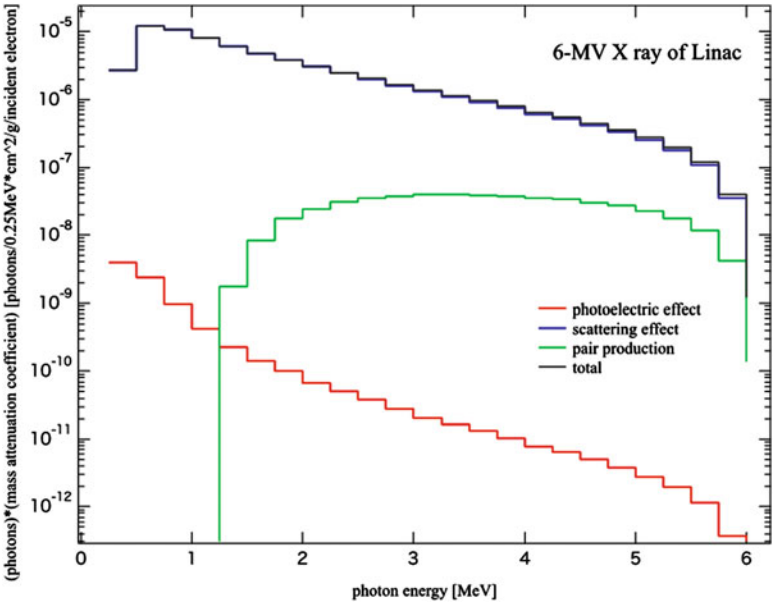

Fig. 3.15 The occupancies for each interaction in the 6-MV X-ray energy spectrum of Linac

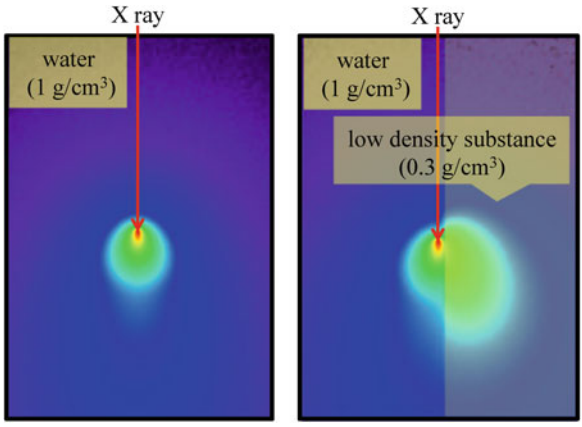

Fig. 3.16 The dose kernel with the 6-MV X-ray energy spectrum of Linac calculated by EGS5 (*left*: in water, *right*: in water/low density substance)

Figure 3.15 shows the product of the energy spectrum of X-rays with 6 MV produced by a Varian Linac and the mass attenuation coefficient for each energy. The value expresses the occupancies for each interaction in the energy spectrum of 6-MV X-rays of the Linac. Figure 3.16 is dose kernel with the 6-MV X-ray energy spectrum of Varian Linac. Dose kernels in homogeneity (water) and inhomogeneity (water / low density substance (30 % of water density)) were calculated by Monte Carlo simulation code: Electron Gamma Shower version 5.0 (EGS5) [3]. And the dose distribution of seven irradiation fields with gantry

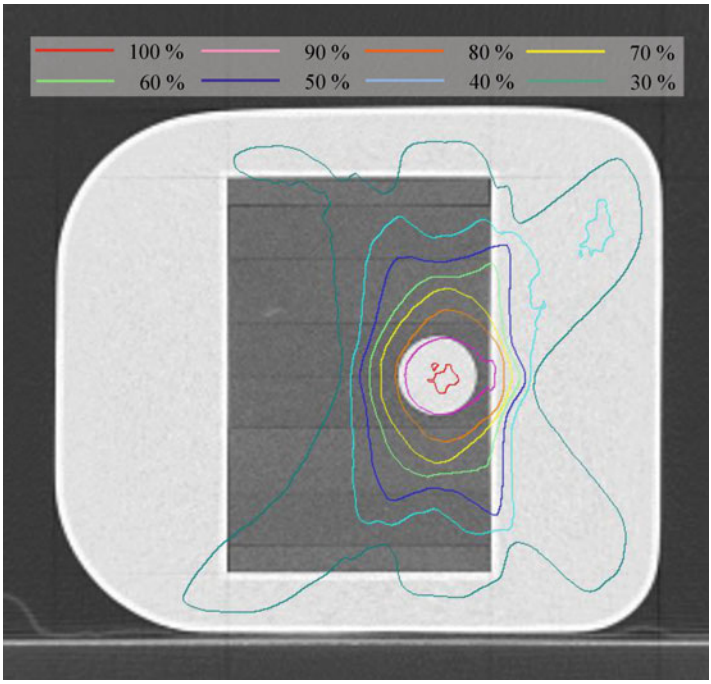

Fig. 3.17 The dose distribution of seven irradiation fields for lung SBRT calculated by EGS5

angles of 5, 50, 135, 175, 220, 280 and 325° in water-tank type lung phantom for lung SBRT [4] calculated by EGS5 is shown in Fig. 3.17. The simulation using the EGS5 was performed with condition of photons of 1.3×10^9, calculation grid size of 1 mm, photon cut-off energy of 10 keV and electron cut-off energy of 200 keV. These simulation data was provided by Medical Physicist S. Kito at Radiation Physics Section, Tokyo Metropolitan Cancer and Infectious Diseases Center Komagome Hospital.

References

1. NIST/XCOM. http://physics.nist.gov/PhysRefData/Xcom/html/xcom1.html
2. Sheikh-Bagheri D, Rogers DWO. Monte Carlo calculation of nine megavoltage photon beam spectra using the BEAM code. Med Phys. 2002;29(3):391–402.
3. Hirayama H, Namito Y, Beilajew AF, Wilderman SJ, Nelson WR The EGS5 Code System. Report SLAC-R-730 and KEK report 2005–8; 2005. http://rcwww.kek.jp/research/egs/egs5_manual/slac730-150228.pdf
4. Nishio T, Shirato H, Ishikawa M, Miyabe Y, Kito S, Narita Y, et al. Design, development of water tank-type lung phantom and dosimetric verification in institutions participating in a phase I study of stereotactic body radiation therapy in patients with T2N0M0 non-small cell lung cancer: Japan Clinical Oncology Group trial (JCOG0702). J Radiat Res. 2014;55(3):600–7.